

Refraction effect in geothermal heat flow due to a 3D prismoid, situated in the substratum of two-layer Earth

Milan HVOŽDARA¹, Dušan MAJCIN¹

¹ Geophysical Institute of the Slovak Academy of Sciences
Dúbravská cesta 9, 845 28 Bratislava, Slovak Republic
e-mail: geofhvoz@savba.sk, geofmadu@savba.sk

Abstract: We present mathematical modelling of the stationary geothermal field for the two-layered Earth which includes a three-dimensional perturbing body below the first layer (in the substratum). The body is in the form of 3D prismoid with sloping side faces, while its upper and lower face are rectangles at the planes $z = z_1, z_2$. The theoretical formulae are based on the generalized theory of the double-layer potential and boundary integral equation (BIE). Special attention is paid to the quadrilateral prismoids bounded by planar skew faces. The numerical calculations were performed for the 3D prismoids (blocks) with thermal conductivity different to the ambient substratum, while the upper face of the prismoid may be in contact with the upper layer. Numerous graphs are shown for the disturbance of the heat flow on the surface of the Earth or inside the first layer.

Key words: geothermics, heat flow refraction, double-layer potential, boundary integral equations, boundary element methods, solid-angle-of-view calculations

1. Introduction

The heat flow from the Earth's interior is of interest in geothermal prospecting based on geothermal models (e.g., *Ljubimova et al., 1983; Chen and Beck, 1991*). The refraction effect in geothermics occurs also due to the presence of a 3D or 2D perturbing body of different thermal conductivity λ_T with respect to the “normal” surrounding horizontally layered medium of thermal conductivity λ_1 if the body is embedded in the 1st layer, $0 < z < h$, or if the body is embedded in the substratum $z > h$ of thermal conductivity λ_2 (Fig. 1). The paper of *Hvoždara and Valkovič (1999)* solved this problem for the rectangular prism and *Hvoždara (2008)* for the prismoid in the first layer. The similar solution for the prismoid situated below the first layer,

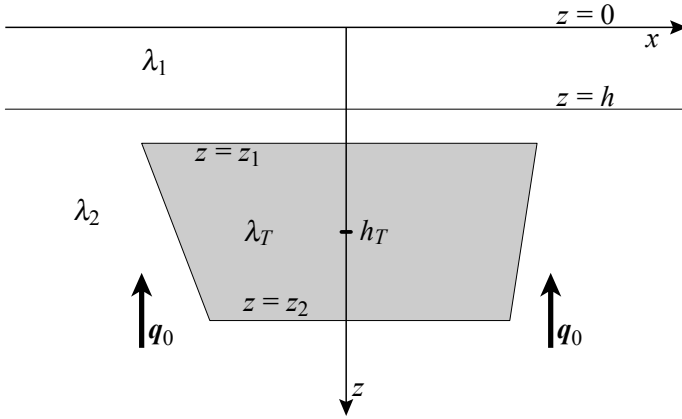


Fig. 1. The x, z cross-section of the 3D perturbing prismoid situated in the substratum of the two layered Earth.

i.e. in the substratum halfspace signed as “2”, is a purpose of this paper. This situation occurs in the geological media when the depression of the first layer penetrates into substratum (graben structure in the sedimentary basin).

A physical qualitative analysis clearly indicates that a well-conducting body ($\lambda_T > \lambda_i, i = 1, 2$) attracts heat flux lines to its interior, while a poorly conducting body ($\lambda_T < \lambda_i$) deflects heat flow lines away. It means that we can expect a positive heat flow anomaly on the surface above the well-conducting body, whereas in the second case a negative heat flow anomaly is expected. Note that the perturbation of the heat flow due to some additional heat sources in the anomalous body is not a subject of this paper although in nature such combined effects have been studied, e.g., in *Ljubimova et al. (1983)*.

Some analytical mathematical models of this effect exist, e.g., *Carslaw and Jaeger (1959)*. The 2D finite difference method has also been applied, e.g., *Majcin (1988)*. For 2D disturbing bodies, embedded in the halfspace, the boundary element method (BEM) has proved to be an effective tool for numerical modeling, e.g., *Chen and Beck (1991)* and also in *Hvoždara and Majcin (2009)*. In this paper we present the BEM theory applied on model situations with prismoid in two layered medium and numerical calculations for this perturbing body, quadrilateral prismoid with upper and

bottom faces parallel with planes $z = 0, h$. The upper face of the prism is rectangle in the plane $z = z_1 \geq h$ and the bottom face is rectangle in the plane $z = z_2, (> z_1)$ as shown in Fig. 1 for the cross-section of the prismoid in the x, z plane.

2. Theoretical background

The theoretical formulation is similar to that in our previous papers *Hvoždara (1982; 2007)*, which solved mathematically similar potential problems of geoelectricity, and to the geothermal problem in *Hvoždara and Valkovič (1999)* and *Hvoždara (2008)*.

The unperturbed stationary temperature field linearly dependent on depth z only, is denoted as $T_1(z)$ for $z \in \langle 0, h \rangle$ and $T_2(z)$ for $z > h$. A simple check shows that the formulae for $T_1(z)$ and $T_2(z)$ are:

$$T_1(z) = q_0 z / \lambda_1, \quad z \in \langle 0, h \rangle, \quad (1)$$

$$T_2(z) = q_0(z - h) / \lambda_2 + q_0 h / \lambda_1, \quad z > h, \quad (2)$$

where q_0 is the unperturbed heat flow density. These functions obey the Laplace equation and continuity of the temperature and heat flow $\lambda \partial T / \partial z$ at the boundary $z = h$.

Due to the presence of perturbing body τ the temperature fields are changed both in layer “1” and substratum “2” by anomalous temperatures $U_1^*(x, y, z)$ and $U_2^*(x, y, z)$. The total temperature fields are:

$$U_1(P) = T_1(P) + U_1^*(P), \quad (3)$$

$$U_2(P) = T_2(P) + U_2^*(P), \quad (4)$$

where $P \equiv (x, y, z)$ is the calculation point. The perturbation parts of $U_1(P)$ and $U_2(P)$ obey the Laplace equations

$$\nabla^2 U_{1,2}^*(P) = 0, \quad (5)$$

with zero limit for $P \rightarrow \infty$ in all directions from the perturbing body. The theoretical analysis of the problem shows that we have to find the regular solution of the boundary value problem for the Laplace equation in media “1”, “2” and in perturbing body τ , where the temperature field is denoted as $U_T(P)$:

$$\nabla^2 U_1^*(P) = 0, \quad \nabla^2 U_2^*(P) = 0, \quad \nabla^2 U_T^*(P) = 0, \quad (6a,b,c)$$

$$\lim_{P \rightarrow \infty} U_1^* = 0, \quad \lim_{P \rightarrow \infty} U_2^* = 0, \quad |U_T(P)| < +\infty, \quad P \in \tau \quad (7a,b,c)$$

$$U_1(P)|_{z=0} = 0, \quad (8)$$

$$U_1(P)|_{z=h} = U_2(P)|_{z=h}, \quad \lambda_1 \frac{\partial U_1(P)}{\partial z} \Big|_{z=h} = \lambda_2 \frac{\partial U_2(P)}{\partial z} \Big|_{z=h}, \quad (9,10)$$

$$U_2(P)|_S = U_T(P)|_S, \quad \lambda_2 \frac{\partial U_2(P)}{\partial n} \Big|_S = \lambda_T \frac{\partial U_T(P)}{\partial n} \Big|_S. \quad (11,12)$$

Here $\partial \dots / \partial n$ denotes the derivative with respect to the outer normal \mathbf{n} to the surface S of the 3D body τ . This potential problem is mathematically similar to the geoelectrical problems solved earlier by *Hvoždara (1982; 1995; 2007)*. The only principal difference is in the boundary condition (8) which says that the temperature on the surface of the Earth is isothermal, this constant temperature can be taken as zero on our (auxiliary) temperature scale. This is expressed by the formulae (1) and (8).

Using an apparatus very similar to the geoelectrical problem mentioned (by means of Green's boundary integral equations in complex media) it can be proved that the solutions of our potential problem is the sum of the unperturbed temperatures and boundary integrals which express the perturbation part of the temperature field. Namely

$$U_1(P) = T_1(P) + \frac{1}{4\pi} \int_S f(Q) \frac{\partial}{\partial n_Q} G_1(P, Q) \, dS_Q, \quad (13)$$

$$U_2(P) = T_2(P) + \frac{1}{4\pi} \int_S f(Q) \frac{\partial}{\partial n_Q} G_2(P, Q) \, dS_Q, \quad (14)$$

$$U_T(P) = \frac{\lambda_2}{\lambda_T} \left[T_2(P) - v_0 + \frac{1}{4\pi} \int_S f(Q) \frac{\partial}{\partial n_Q} G_2(P, Q) \, dS_Q \right] + v_0, \quad (15)$$

where $G_1(P, Q)$ and $G_2(P, Q)$ are the Green's functions and $\partial G_{1,2}(P, Q) / \partial n_Q$ denote their derivatives with respect to the outer normal \mathbf{n}_Q on the surface of the perturbing body. The surface S of the perturbing body is assumed

to be piecewise smooth in Lyapunov's sense. The function $f(Q)$ expresses the distribution of the double-layer density distributed on surface S , it must be determined by solving the boundary integral equation as will be shown next. Point $Q \equiv (x', y', z')$ is the moving point shifted along S . A constant v_0 is the mean value of the unperturbed temperature $T_2(P)$ on the surface S :

$$v_0 = \frac{1}{S} \int_s T_2(P) dS_P. \quad (16)$$

3. The Green's functions and the boundary integral equation

Boundary conditions (7a,b,c) and (8)–(10) can be fulfilled by the proper determination of Green's functions. These Green's functions G_1, G_2 must obey 3D partial Poisson's or Laplace's equation:

$$\nabla^2 G_1(P, Q) = 0, \quad z \in \langle 0, h \rangle \quad (17)$$

and

$$\nabla^2 G_2(P, Q) = -4\pi\delta(P, Q), \quad z > h, \quad (18)$$

where $\delta(P, Q)$ is a 3D Dirac function whose pole is at point $Q \equiv (x', y', z') \in \tau$. These Green's functions satisfy similar boundary conditions on $z = 0$, and $z = h$ as the temperature field:

$$G_1(P, Q)|_{z=0} = 0, \quad (19)$$

$$[G_1(P, Q) - G_2(P, Q)]_{z=h} = 0, \quad (20a)$$

$$[\lambda_1 \partial G_1(P, Q) / \partial z]_{z=h} = [\lambda_2 \partial G_2(P, Q) / \partial z]_{z=h}, \quad (20b)$$

$$\lim_{P \rightarrow \infty} G_{1,2}(P, Q) \Big| = 0. \quad (21)$$

Physically $G_1(P, Q)$ or $G_2(P, Q)$ represents the temperature of the point heat source located at point $Q \in \text{"2"}$ and calculated for point P in the upper layer ($G_1(P, Q)$) or in substratum $G_2(P, Q)$. But the common source multiplier $q_0/(4\pi\lambda_2)$ is replaced by 1 in order to satisfy the Poisson's equation (18), which has the non-trivial solution:

$$g_2(P, Q) = 1/R = \left[(x - x')^2 + (y - y')^2 + (z - z')^2 \right]^{-1/2}, \tag{22}$$

since $\nabla^2(1/R) = -4\pi\delta(P, Q)$. The remaining part of $G_2(P, Q)$, i.e. $\tilde{G}_2(P, Q)$ satisfies the Laplace equation.

Let us choose an auxiliary cylindrical system (r, φ, z) whose polar axis runs through point Q perpendicularly to boundaries $z = 0$ and $z = h$. Green’s functions will then be independent of azimuthal angle φ and the Laplace equation for harmonic functions $\tilde{G}_1(P, Q)$ and $\tilde{G}_2(P, Q)$ takes the form:

$$\frac{\partial^2 \tilde{G}}{\partial r^2} + \frac{1}{r} \frac{\partial \tilde{G}}{\partial r} + \frac{\partial^2 \tilde{G}}{\partial z^2} = 0. \tag{23}$$

The particular solution can be found by applying the method of separation of variables:

$$\tilde{G}(r, z) = J_0(tr) \begin{cases} e^{tz} \\ e^{-tz} \end{cases}, \tag{24}$$

where $J_0(tr)$ is the Bessel function of the 1st kind and zero order. $G_1(r, z)$ and $G_2(r, z)$ can be expressed as:

$$G_1(r, z) = \int_0^\infty A_1 \operatorname{sh}(tz) J_0(tr) dt, \tag{25}$$

$$G_2(r, z) = \left[r^2 + (z - z')^2 \right]^{-1/2} + \int_0^\infty A_2 e^{-tz} J_0(tr) dt. \tag{26}$$

It is clear that the radial coordinate r is expressed in the original Cartesian co-ordinate system as:

$$r = \left[(x - x')^2 + (y - y')^2 \right]^{1/2}. \tag{27}$$

It can be easily verified that the Green’s function $G_1(P, Q)$ obeys the boundary equation (19) at surface $z = 0$. In order to find functions A_1 and A_2 , we express $1/R$ in terms of the Weber-Lipschitz integral:

$$\frac{1}{R} = \int_0^\infty e^{-t|z-z'|} J_0(tr) dt, \tag{28}$$

accounting that at $z \rightarrow h$ we must put $|z - z'| = z' - z$, since $z' > z$. In order to satisfy the boundary conditions at $z = h$ we obtain the system of linear equations for A_1, A_2 :

$$\begin{aligned} A_1 \operatorname{sh}(th) - A_2 e^{-th} &= e^{-t(z'-h)}, \\ A_1 \operatorname{ch}(th) + (\lambda_2/\lambda_1) A_2 e^{-th} &= (\lambda_2/\lambda_1) e^{-t(z'-h)}. \end{aligned} \tag{29}$$

We can easily solve this system:

$$A_1 = 2(1+k)e^{-tz'} [1 - ke^{-2th}]^{-1}, \tag{30}$$

$$A_2 = (k - e^{-2th})e^{-t(z'-2h)} [1 - ke^{-2th}]^{-1}, \tag{31}$$

where

$$k = (1 - \lambda_1/\lambda_2)/(1 + \lambda_1/\lambda_2). \tag{32}$$

Now we can use the well-known expansion of factor $[1 - ke^{-2th}]^{-1}$ into the infinite geometrical series:

$$[1 - ke^{-2th}]^{-1} = \sum_{n=0}^\infty k^n e^{-2nth}, \tag{33}$$

since $|ke^{-2th}| < 1$. Using the Weber-Lipschitz integral in (25) and (26) we obtain convenient expressions of $G_1(P, Q)$ and $G_2(P, Q)$:

$$G_1(P, Q) = (1+k) [R^{-1} - R_+^{-1}] + (1+k) \sum_{n=1}^\infty k^n [R_{1n}^{-1} - R_{2n}^{-1}], \tag{34}$$

$$G_2(P, Q) = R^{-1} - (1 - k^2)R_+^{-1} + kR_h^{-1} - (1 - k^2) \sum_{n=1}^\infty k^n R_{2n}^{-1}, \tag{35}$$

where

$$\begin{aligned} R_+^{-1} &= [r^2 + (z + z')^2]^{-1/2}, & R_h^{-1} &= [r^2 + (2h - z - z')^2]^{-1/2}, \\ R_{1n}^{-1} &= [r^2 + (z' - z + 2nh)^2]^{-1/2}, & R_{2n}^{-1} &= [r^2 + (z' + z + 2nh)^2]^{-1/2}. \end{aligned}$$

Note that if $\lambda_2 = \lambda_1$, i.e. $k = 0$ we obtain a simple two-term Green's function: $R^{-1} - R_+^{-1}$ for the whole halfspace $z > 0$. Now we can derive the boundary integral equation (B.I.E) for determining the function $f(P)$, which is necessary to calculate the temperatures (13)–(15). Assume that perturbing body τ is not in contact with any of its faces (parts of boundary S) having planar boundaries $z = 0$ or $z = h$. If point P approaches the surface (S) from inside ($P \rightarrow S_-$) or from outside ($P \rightarrow S_+$), singularity in $G_2(P, Q)$ occurs due to the well-known term R^{-1} . This singularity can be treated using the classical theory of the potential double layer (e.g., *Hvoždara (1995)*). After applying the limit transition (13) yields

$$\lim_{P \rightarrow S_+} U_2(P) = T_2(P) + \frac{1}{2}f(P) + \frac{1}{4\pi} \int_S f(Q) \frac{\partial}{\partial n_Q} G_2(P, Q) dS_Q, \quad P \in S, \quad (36)$$

where the backward slash on the integral sign denotes an integration in the principal sense, i.e. the integration of the part with $\partial R^{-1} / \partial n_Q$ is performed over the whole surface S with the exception of the infinitesimally small area ΔS_p around point $P \in S$, where $\partial R^{-1} / \partial n_Q$ has a integrable singularity. The integration of this singular term on ΔS_p resulted in the contribution $\frac{1}{2}f(P)$ in Eq. (36).

A similar limit transition in (15) from the interior of S reads ($P \rightarrow S_-$):

$$\begin{aligned} \lim_{P \rightarrow S_-} U_T(P) &= \\ &= \frac{\lambda_2}{\lambda_T} \left[T_2(P) - v_0 - \frac{1}{2}f(P) + \frac{1}{4\pi} \int_S f(Q) \frac{\partial}{\partial n_Q} G_2(P, Q) dS_Q \right] + v_0. \end{aligned} \quad (37)$$

The negative sign of term $\frac{1}{2}f(P)$ is well-known in the theory of the classical double-layer potential as a discontinuity of the double-layer potential on the supporting surface S . According to the boundary condition (11) the r.h.s. of Eqs. (36) and (37) must be equal, after some algebra we obtain the BIE for calculation of the double-layer density $f(P)$:

$$f(P) = 2\beta [T_2(P) - v_0] + \frac{\beta}{2\pi} \int_S f(Q) \frac{\partial}{\partial n_Q} G_2(P, Q) dS_Q, \quad P \in S \quad (38)$$

where $\beta = (1 - \lambda_T / \lambda_2) / (1 + \lambda_T / \lambda_2)$. Since the normal derivative of the kernel $\partial^2 R^{-1} / \partial n_Q \partial n_p$ is continuous on the supporting surface S we can

easily check the validity of the boundary condition (12).

The boundary integral solution of our problem is now completed. The BIE (38) can only be analytically solved in some simple cases, but for the block body it must be treated numerically, in analogy (e.g., *Brebbia et al., 1984; Hvoždara, 2007*) with the approach using the boundary element methods (BEM).

For the practical purpose it is important to study also the case when the body τ touches to its upper face S_h : ($z = z_1$) the planar boundary $z = h$, which approximates the depression of the sedimentary basin. In this case there are two singular terms in $G_2(P, Q)$ for points $P \in S_h$; those are R^{-1} and kR_h^{-1} . The analysis like that in the paper by *Hvoždara and Valkovič (1999)* will give modified BIE instead of (38):

$$f(P) = 2\alpha [T_2(P) - v_0] + \frac{\alpha}{2\pi} \int_S f(Q) \frac{\partial}{\partial n_Q} G_2(P, Q) dS_Q, \quad (39)$$

$$\text{where } \alpha = \begin{cases} \beta & \text{if } P \notin S_h, \\ \beta/(1 - k\beta) & \text{if } P \in S_h. \end{cases}$$

The double slash on the integral sign of BIE (39) indicates that there are omitted contributions due to two singular terms (R^{-1} and kR_h^{-1}) for $P \in S_h$, while for $P \notin S_h$ there are omitted only contributions due to R^{-1} .

4. Calculation of the solid angle of view for the triangle and quadrangle subarea with general orientation of its normal

The crucial part of numerical calculations of BIE consists of the calculation of integrals with the kernel of type of the double-layer potential: $\mathbf{n}' \cdot (\mathbf{r} - \mathbf{r}') |\mathbf{r} - \mathbf{r}'|^{-3}$ over a small subsurface ΔF_j which is the part of surface S of the perturbing body τ . Then the basic task is in the reliable calculation of such integrals for the triangle planar subarea ΔF_j with corners ABC as shown in Fig. 2:

$$\Delta A_j = \int_{\Delta F_j} \frac{\mathbf{n}' \cdot (\mathbf{r} - \mathbf{r}')}{|\mathbf{r} - \mathbf{r}'|^3} dS_Q = -\Delta \Omega_j, \quad (40)$$

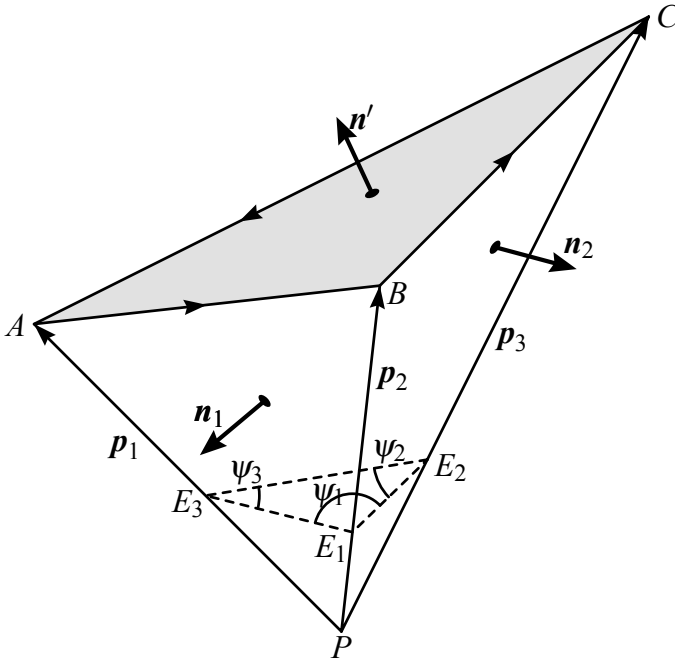


Fig. 2. The parameters for calculation of solid angle of view onto triangular subarea.

where $Q(\mathbf{r}')$ is the variable point on the subarea ΔF_j . By using the classical knowledge on the Gaussian integral for the double-layer potential, we see that $\Delta\Omega_j$ is the solid angle of view from the point $P(\mathbf{r})$ onto planar triangle subarea ΔF_j with outer normal $\mathbf{n}' \equiv (n'_x, n'_y, n'_z) \equiv \mathbf{n}_Q$. The formula given by Ivan (1994) is reliable for the calculation of ΔA_j and we used it in previous papers Hvoždara (2007; 2008). Later, we found simpler guide for calculation ΔA_j published in the paper Guptasarma and Singh (1999). We adopted their method in the present paper.

Geometrical situation of the point of view P and triangular subarea with vertices ABC is depicted in Fig. 2. The points PABC form a tetrahedron with vertex P and triangular base ABC. The position of vertices ABC with respect to the point P is given by vectors $\mathbf{p}_1, \mathbf{p}_2, \mathbf{p}_3$ while circulation around the triangle is counterclockwise. The normal \mathbf{n}' onto triangular subarea is of unit length and has fixed orientation for the whole triangle ABC. Using the basic theory of spherical trigonometry we can calculate the solid angle

of view from the point P onto triangular area ABC by means of Girard's formula:

$$\Delta\Omega_j = (\psi_1 + \psi_2 + \psi_3 - \pi) \cdot inp. \tag{41}$$

Here ψ_1 is the inner angle between planes PAB and PBC , ψ_2 is similar angle between PBC and PCA and finally the third angle ψ_3 is defined for planes PCA and PAB . These angles are depicted on the dashed triangle E_1, E_2, E_3 in Fig. 2. The number $inp = \pm 1$ is signum of the scalar product $\mathbf{p}_1 \cdot \mathbf{n}'$. If this scalar product is zero, then $inp = 0$ and $\Delta\Omega_j = 0$ because the point P lies in the plane which contains also subarea ABC , so the solid angle of view must be zero. Let us define outer normals $\mathbf{n}_1, \mathbf{n}_2, \mathbf{n}_3$ on the faces PAB, PBC and PCA of the tetrahedron. These vectors are of unit length and can be calculated by the vector products and their absolute values:

$$\begin{aligned} \mathbf{n}_1 &= (\mathbf{p}_2 \times \mathbf{p}_1) / |\mathbf{p}_2 \times \mathbf{p}_1|, \\ \mathbf{n}_2 &= (\mathbf{p}_3 \times \mathbf{p}_2) / |\mathbf{p}_3 \times \mathbf{p}_2|, \\ \mathbf{n}_3 &= (\mathbf{p}_1 \times \mathbf{p}_3) / |\mathbf{p}_1 \times \mathbf{p}_3|. \end{aligned} \tag{42}$$

Now consider the situation at the edge \mathbf{p}_2 where the planes PAB and PBC intersect, forming the angle ψ_1 . According to the scheme in the Fig. 3 it is clear that $\cos \psi_1$ can be calculated as:

$$\cos \psi_1 = \mathbf{n}_1 \cdot (-\mathbf{n}_2) = -\mathbf{n}_1 \cdot \mathbf{n}_2. \tag{43}$$

Similar scalar products give also:

$$\cos \psi_2 = \mathbf{n}_2 \cdot (-\mathbf{n}_3) = -\mathbf{n}_2 \cdot \mathbf{n}_3, \quad \cos \psi_3 = \mathbf{n}_3 \cdot (-\mathbf{n}_1) = -\mathbf{n}_3 \cdot \mathbf{n}_1. \tag{44}$$

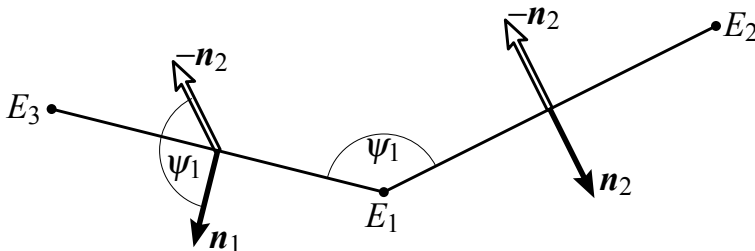


Fig. 3. Scheme of calculation of angle ψ_1 by means of scalar product \mathbf{n}_1 and $-\mathbf{n}_2$.

From the definition of the tetrahedron it is clear that each angle ψ_i is less than π , so their values can be calculated by the standard subroutine arcos (ACOS) in Fortran. By substitution into formula (41) we have $\Delta\Omega_j$. Note that the value $\psi_1 + \psi_2 + \psi_3 - \pi$ is known as an excess of spherical triangle. Using this algorithm we can calculate integrals of the type:

$$v_{ij} = \int_{\Delta S_j} \frac{(\mathbf{r}_i - \mathbf{r}') \cdot \mathbf{n}'_j}{|\mathbf{r}_i - \mathbf{r}'|^3} dS_Q = -\Delta\Omega_{ij}, \tag{45}$$

where \mathbf{r}_i is positional vector for the point of view $P(\mathbf{r}_i)$ and ΔS_j is triangular subarea with outer normal \mathbf{n}'_j and point $Q(\mathbf{r}')$ is moving on the subarea.

It must be stressed that this algorithm, when applied to the whole closed boundary S (with piecewise continuous normal \mathbf{n}_Q), must give with high precision, better than 10^{-3} , the well known fundamental values of the Gauss integral:

$$\int_S \frac{\partial}{\partial n_Q} \frac{1}{|\mathbf{r} - \mathbf{r}'|} dS_Q = \int_S \frac{\mathbf{n}' \cdot (\mathbf{r} - \mathbf{r}')}{|\mathbf{r} - \mathbf{r}'|^3} dS_Q = \begin{cases} 0, & P(\mathbf{r}) \in \text{Ext}(S) \\ -2\pi, & P(\mathbf{r}) \in S \\ -4\pi, & P(\mathbf{r}) \in \text{Int}(S) \end{cases} . \tag{46}$$

It is clear that if the closed surface is divided into large number M of subareas ΔS_j then formula (46) gives the check values:

$$\sum_{j=1}^M \Delta\Omega_{ij} = \begin{cases} 0, & P(\mathbf{r}_i) \in \text{Ext}(S) \\ 2\pi, & P(\mathbf{r}_i) \in S \\ 4\pi, & P(\mathbf{r}_i) \in \text{Int}(S) \end{cases} . \tag{47}$$

These check values must be verified at numerical solution of the BIE, as well as at calculation of $U_1(P)$, $U_2(P)$. For the calculation of integral (40) by means of (41) we successfully realized our original subroutine SLAGUP3 and tested it for the prismoids, like that we show in Fig. 1. We have found that the subdivision of the sloped planar faces of the prismoid into a set of triangle subareas is rather awkward and leads to a large number of subareas. So we decided to improve the algorithm into quadrilateral subareas ΔS_j , with four vertices T_1, T_2, T_3, T_4 , while normal \mathbf{n}_Q is constant for the whole face of the prismoid. In this manner we decrease the number of subareas onto one half in comparison with triangle case ΔF_j . The calculation

of the solid angle of view for the quadrangle is performed by application of SLAGUP3 for triangle $\Delta T_1 T_2 T_3$ and then for $\Delta T_3 T_4 T_1$. The scheme of subdivision for some of six quadrilateral faces of the prismoid is shown in Fig. 4. The subroutine SLAGUP4 gives values of the Gauss integral (46) i.e. $(-4\pi, -2\pi, 0)$ with accuracy of at least 4 decimal digits. Let us note

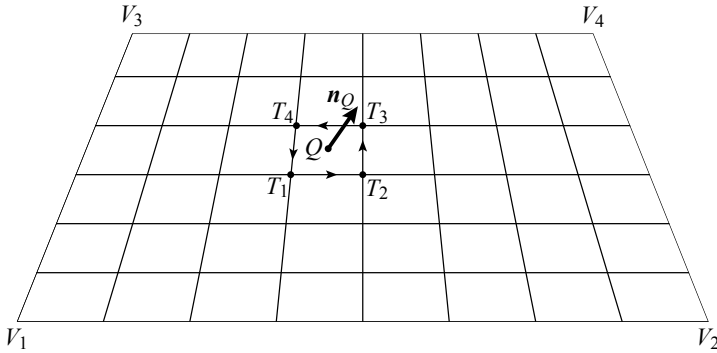


Fig. 4. Scheme of the quadrilateral face of the prismoid and its subdivision into quadrilateral subareas like $T_1 T_2 T_3 T_4$. Note that opposite sides are divided into equal number of intervals, e.g. sides V_1, V_2 and V_3, V_4 have 8 segments.

that the demands on the computing time and memory were greater than for the similar problem with rectangular faces, because of the more complicated algorithm of calculations of the solid angle $\Delta\Omega_j$. In the numerical calculations it is necessary to store x, y, z coordinates of vertices for each subarea, as well as coordinates of its centre, which increases demands on computer time and memory. Also, we note that components of \mathbf{n}_Q are the same for every subarea ΔF_j of the quadrangle face of the prismoid.

5. Numerical calculations and discussion

The numerical calculations were performed in a similar way as in *Hvoždara (1995; 2007; 2008)*, noting that the Green’s function $G_1(P, Q)$, $G_2(P, Q)$ are given by the infinite series (34) and (35). Nevertheless, the principal terms are again R^{-1} , R_+^{-1} and $R_h^{-1} = [r^2 + (2h - z - z')^2]^{-1/2}$. The special cases when the perturbing body touches the planar boundary $z = h$ of the

layer “1” must be treated by the BIE (39). The BIE (38) can be solved by the collocation method. It means that the surface S of the perturbing body is discretized into M quadrilateral subareas ΔS_j whose centres we denote as P_m or Q_j . It is also assumed that each subarea is small enough to put $f(Q) = f(Q_j) = \text{const}$ on it. So we introduce the constant approximation of an unknown function $f(Q)$ on ΔS_j . Putting the number M sufficiently large, we can express the BIE (38) in its discretized form:

$$f(P_m) = 2\gamma[V_1(P_m) - v_0] + \sum_{j=1}^M f(Q_j)W(P_m, Q_j), \quad m = 1, 2, \dots, M. \quad (48)$$

Here $\gamma = \beta$ if the body does not touch at the point P_m the planar boundary of the upper layer and attains slightly changed values α as given in (39) if the prismoid is in contact with planar boundary $z = h$. The weighting coefficients $W(P_m, Q_j)$ are given by the formula:

$$W(P_m, Q_j) = \frac{\gamma}{2\pi} \int_{\Delta S_j} \frac{\partial}{\partial n_Q} G_2(P_m, Q) dS_Q. \quad (49)$$

The integration in the principal value sense was explained in comment to the formulae (38) and (39). It follows that $W(P_m, Q_j)$ cannot be infinite even if $P_m \equiv Q_m$.

In fact, the formula (48) is the system of M linear equations for the unknown values $f(Q_j)$. This system can be expressed as follows:

$$\sum_{j=1}^M [\delta_{mj} - W(P_m, Q_j)] f(Q_j) = 2\gamma[V_1(P_m) - v_0], \quad m = 1, 2, \dots, M, \quad (50)$$

where δ_{mj} is the Kronecker symbol. Then the system of equations can be solved using known methods of linear algebra. Once the system (50) is solved, we can calculate the temperature field and other geothermal characteristics, namely the vertical component of the heat flow density q_z or its anomaly Δq_z .

We checked this algorithm for a prismoid with rectangular bottom and top face while side faces are quadrilaterals. The upper face of the prismoid is a rectangle and it lies at the depth $z_1 \geq h$, the bottom rectangle is at the depth $z_2 > z_1$, so the prismoid is situated in the substratum. The central

depth plane of the prismoid is $h_T = (z_1 + z_2)/2$. This block is situated in the substratum with thermal conductivity λ_2 , the thickness surface layer being h . The thermal conductivity of the prismoid is set to $\lambda_T = \lambda_1$, as some model of penetration (depression) of the upper medium into substratum and we suppose $\lambda_2 = 0.4\lambda_1$, i.e. substratum is less conductive in comparison to prismoid.

The subdivision of each face was performed by introducing the numbers of division (> 5) for edges of each pair of opposite sides of the trapezoid, which is a general form of some face of the prismoid as shown Fig. 4. The x, y, z coordinates of vertices for each subarea in the form of quadrangle are stored, since they are used as vertices T_1, T_2, T_3, T_4 for repeated call of calculations of the solid angle of view by means of subroutine SLAGUP4. The direction cosines of the unit normal \mathbf{n}_Q remain constant for each trapezoidal planar face of the prismoid. Let us note that for solving the system (50) for each of the central points P_m there must be calculated weighting coefficients $W(P_m, Q_j)$ for all sets of point Q_j , while in the Green's function we must treat by using SLAGUP4 at least contributions from R^{-1} , and also from R_h^{-1} . If we choose the subdivision of each trapezoidal face into 64 quadrangle subareas, we obtain $6 \times 64 = 384 = M$ surface elements ΔS_j , which contribute into the summation approximation of the boundary integrals. After solution of linear equation system (50) we obtain $f(Q_j)$ for individual subareas and then we calculate the temperature field in the plane $y = 0$ for equidistant levels $z \in \langle 0, 1.2z_2 \rangle$ using formula (13) with the summation approximation of the boundary integral. For those selected z -levels we also calculated the vertical heat flow density q_z by the difference of temperatures at neighbouring levels z :

$$q_z(x, y, z_j) = \lambda_1 [U_1(x, y, z_j + \Delta z) - U_1(x, y, z_j)] / \Delta z, \quad (51)$$

where $\Delta z = h/20$. For the surface $z = 0$ there is

$$q_z(x, y, 0) = \lambda_1 U_1(x, y, \Delta z) / \Delta z, \quad (52)$$

in view of the boundary condition (8). We calculated a number of models, but here we present graphs for three models only. The first model is for the prismoid in contact with the layer ($z_1 = h$) and in the second model prismoid is slightly separated $z_1 = 1.2h$. In both cases the thickness of the prismoid is quite large $z_2 - z_1 = h$ and ratio $\lambda_T/\lambda_2 = 2.5$ while $\lambda_1 = \lambda_T$.

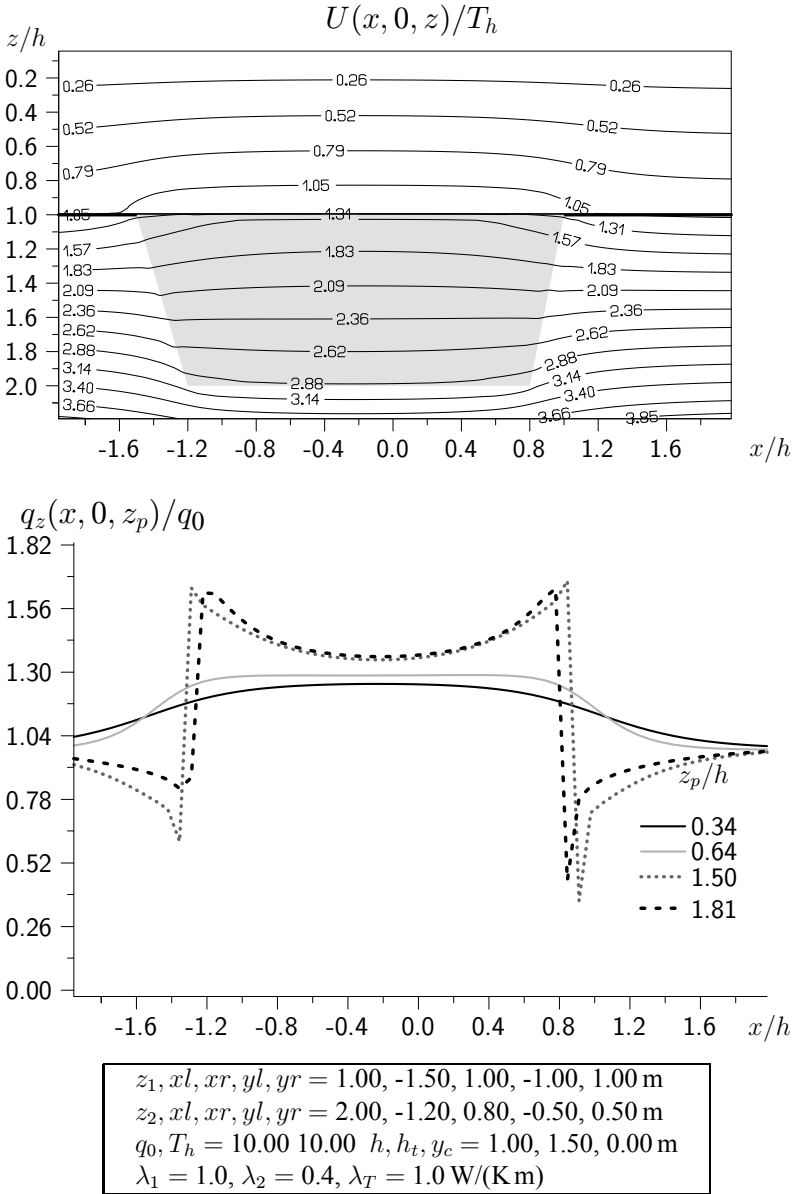


Fig. 5a. Isolines of temperature (top) and profile curves of the vertical heat flow (bottom) in the plane $y = 0$ for the prismoid in the substratum, which is in contact with the boundary $z = h$ and parameters given in the bottom box table ($\lambda_T/\lambda_2 = 2.5$).

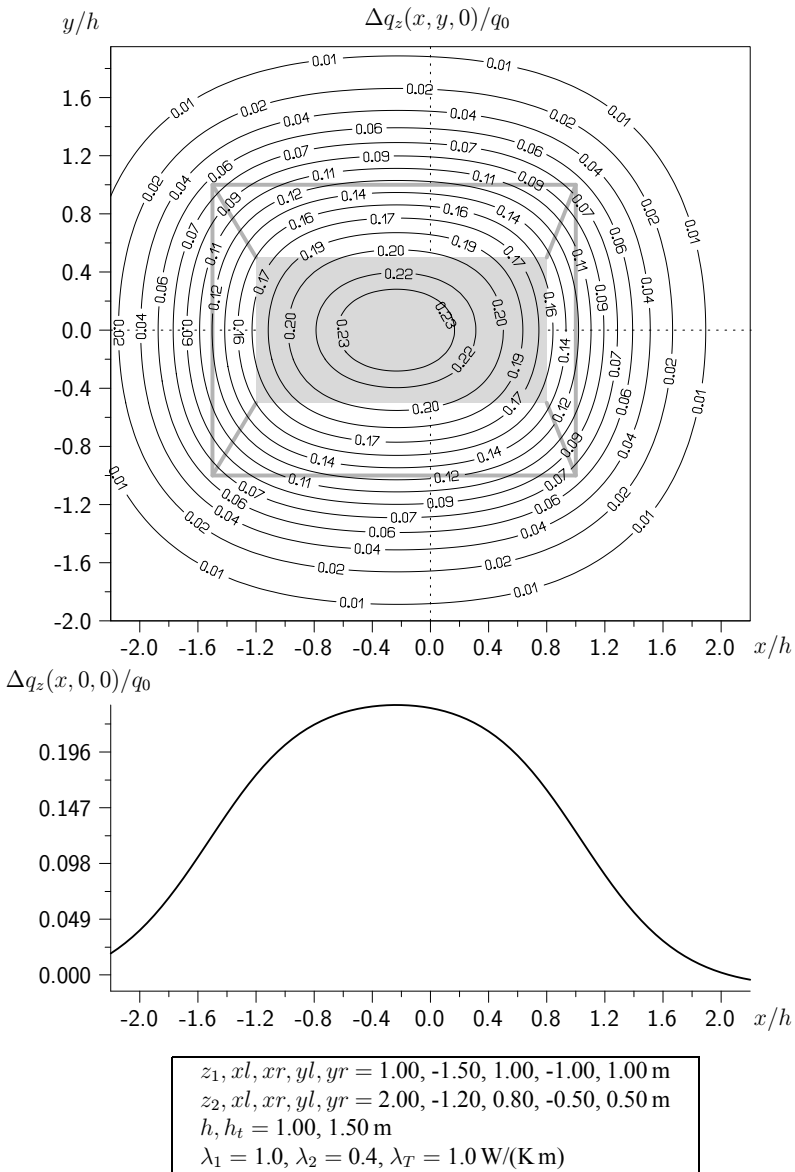


Fig. 5b. Isolines and profile curve of q_z/q_0 at the surface $z = 0$ for prismoid with $\lambda_T/\lambda_2 = 2.5$. There is also depicted projection of the prismoid with sloped faces. The gray rectangle is projection of the bottom face.

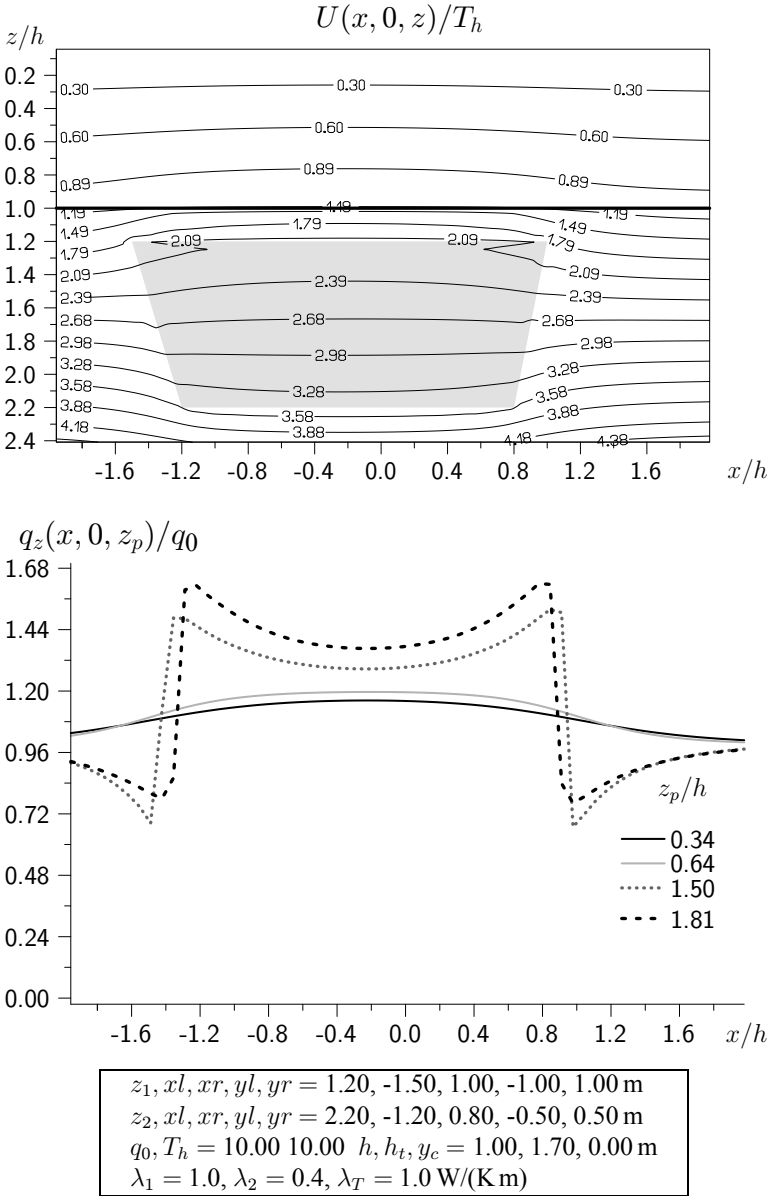


Fig. 6a. Isolines of temperature (top) and profile curves of the vertical heat flow (bottom) in the plane $y = 0$ for the prismoid in the substratum, which is below the upper layer, $z_1 = 1.2h$ and parameters given in bottom box table ($\lambda_T/\lambda_2 = 2.5$).

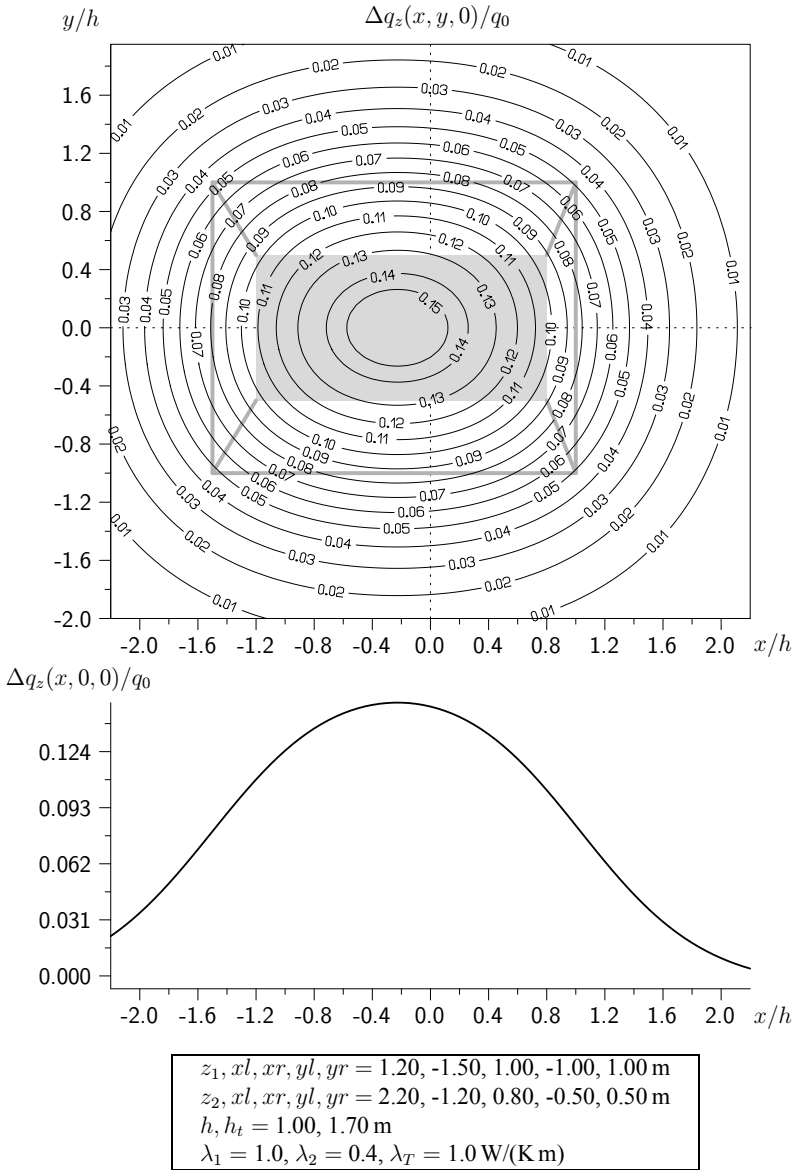


Fig. 6b. Isolines and profile curve of q_z/q_0 at the surface $z = 0$ for prismoid with $\lambda_T/\lambda_2 = 2.5$ and buried below the first layer $z_1 = 1.2h$. There is also depicted projection of the prismoid with sloped faces. The gray rectangle is projection of the bottom face.

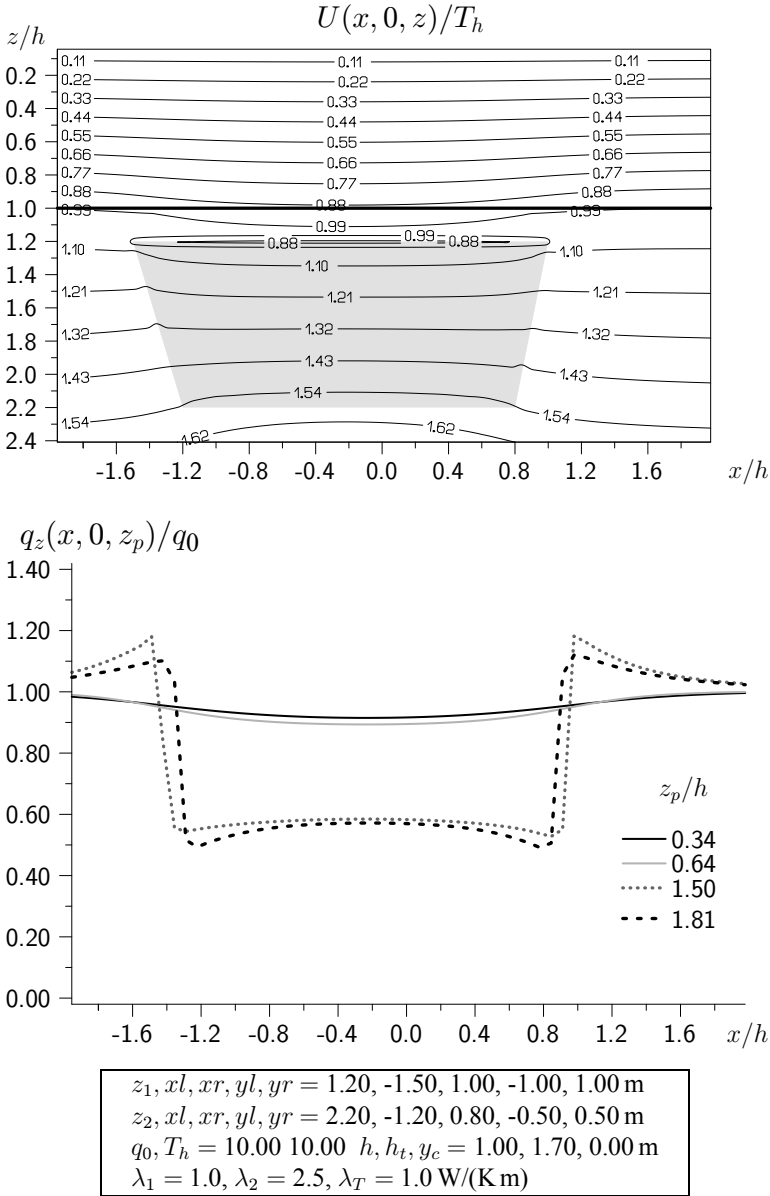


Fig. 7a. Isolines of temperature (top) and profile curves of the vertical heat flow (bottom) in the plane $y = 0$ for the prismoid in the substratum, which is below the upper layer, $z_1 = 1.2h$ and parameters given in bottom box table ($\lambda_T/\lambda_2 = 0.4$).

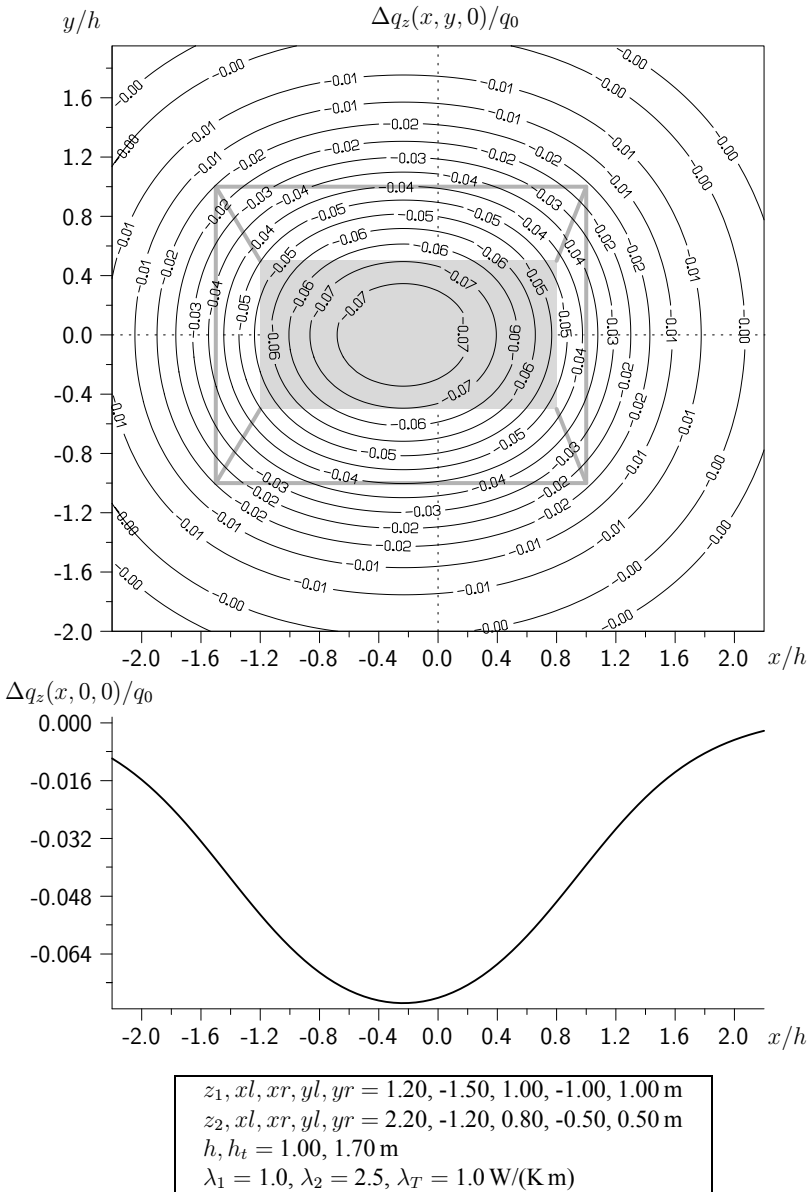


Fig. 7b. Isolines and profile curve of q_z/q_0 at the surface $z = 0$ for prismoid with $\lambda_T/\lambda_2 = 0.4$ and buried below the first layer $z_1 = 1.2h$. There is also depicted projection of the prismoid with sloped faces. The gray rectangle is projection of the bottom face.

The third model is geometrically identical with the second one, but the ratio $\lambda_T/\lambda_2 = 0.4$.

The results for the first model are presented in Figs. 5a,b. In Fig. 5a we present the temperature field $U(x, 0, z)$ normalized to the normal temperature on the bottom of the layer $T_h = q_0 h/\lambda_1$. The isolines of $U(x, 0, z)/T_h$ can be considered as isotherms in the layer “1”, part of substratum “2” and also in the prismoid for the plane $y = 0$. We can see that till the depth $z/h = 0.8$ the course is almost parallel with the lines $z = \text{const}$, but in the neighbourhood of the prismoid faces these are considerably deformed. In the bottom part of Fig. 5a we also present the profile curves of $q_z(x, 0, z_p)/q_0$ calculated for 4 values of z_p/h . The first two smooth profile curves belong to depths $z_p/h < 1$, i.e. inside the layer “1”. The graphs for $z_p/h = 1.5, 1.81$ are marked with discontinuities at the sloped faces of the prism. In Fig. 5b, we plotted the map of the surface heat flow anomaly, with the q_z calculated by the formula (52). We see that the heat flow anomaly attains almost 22% of q_0 . In this figure we depicted also the projection of the bottom rectangle $z = z_2$ (gray) and larger upper rectangle. The parameters of the model prismoid are given in the box tables in each figure, namely: for the larger upper rectangle face of the prismoid at the depth z_1 , xl, xr, yl, yr are x, y coordinates (left, right) of the corners; similar values z_2, xl, xr, yl, yr concern the bottom (smaller) rectangle of the prismoid at the depth z_2 . In each table there are also given values used for normalization: $T_h = 10\text{ K}$, $q_0 = 10\text{ W/m}^2$, $h = 1\text{ m}$ and also used values of thermal conductivities ($\lambda_1, \lambda_2, \lambda_T$). In Figs. 6a–b there are presented characteristics of the temperature field similar to Figs. 5a–b. We can see that even a small separation of the prismoid from the layer causes considerable differences in calculated fields. Figs. 7a,b present resulting graphs for the model of high conductive substratum “2” with low conductive prismoidal inclusion ($\lambda_T/\lambda_2 = 0.4$ and also layer “1” is of low conductivity $\lambda_1/\lambda_2 = 0.4$). In Fig. 7a we can see different course of isotherms and also of profile curves of q_z/q_0 . The map of surface heat flow in Fig. 7b shows a negative anomaly. Finally we can state that we have proved applicability of BIE method also for deeply buried prismoids of more general shape than the rectangular prism.

Acknowledgments. The author is grateful to the Slovak Grant Agency VEGA for partial support of the work by means of projects No. 2/0169/09 and No. 2/0107/09.

References

- Brebbia C. A., Telles J. C. F., Wrobel L. C., 1984: Boundary element techniques. Springer Verlag, Berlin.
- Carslaw H. S., Jaeger J. C., 1959: Conduction of heat in solids. Clarendon Press, Oxford.
- Chen Y., Beck A. E., 1991: Application of the boundary element method to a terrestrial heat flow problem. *Geophys. J. Int.*, **107**, 25–35.
- Guptasarma D., Singh B., 1999: New scheme for computing the magnetic field resulting from uniformly magnetized arbitrary polyhedron. *Geophysics*, **64**, 70–74.
- Hvoždara M., 1982: Potential field of a stationary electric current in a stratified medium with a three-dimensional perturbing body. *Studia Geophys. Geodaet.*, **26**, 160–172.
- Hvoždara M., 1995: The boundary integral calculation of the D.C. geoelectric field due to a point current source on the surface of 2-layered earth with a 3D perturbing body, buried or outcropping. *Contr. Geoph. Inst. Slov. Acad. Sci.*, **25**, 7–25.
- Hvoždara M., Valkovič L., 1999: Refraction effect in geothermal heat flow due to a 3D prism in a two-layered Earth. *Studia Geophys. Geodaet.*, **43**, 407–426.
- Hvoždara M., 2007: The boundary integral numerical modelling of the D.C. geoelectric field in a two-layered earth with a 3D block inhomogeneity bounded by sloped faces. *Contrib. Geophys. Geod.*, **37**, 1, 1–22.
- Hvoždara M., 2008: Refraction effect in the heat flow due to a 3-D prismoid, situated in a two-layered earth. *Contrib. Geophys. Geod.*, **38**, 4, 371–390.
- Hvoždara M., Majcin D., 2009: Geothermal refraction for a 2-D body of polygonal cross-section buried in the two-layered Earth. *Contrib. Geophys. Geod.*, **39**, 4, 301–323.
- Ivan M., 1994: Upward continuation of potential fields from a polyhedral surface. *Geophys. Prosp.*, **42**, 391–404.
- Ljubimova E. A., Ljuboschits V. M., Parfenyuk O. I., 1983: Numerical model of temperature fields in the Earth. Nauka, Moskva (in Russian).
- Majcin D., 1988: Computation of the temperature distribution along the DSS profiles running through Slovakia. *Contr. Geoph. Inst. Slov. Acad. Sci.*, **18**, 38–57.